AJNR

Proton MR Spectroscopy of Tumefactive Demyelinating Lesions

Amit M. Saindane, Soonmee Cha, Meng Law, Xiaonan Xue, Edmond A. Knopp and David Zagzag

AJNR Am J Neuroradiol 2002, 23 (8) 1378-1386
http://www.ajnr.org/content/23/8/1378

AJNR Am J Neuroradiol 23:1378–1386, September 2002

Proton MR Spectroscopy of Tumefactive Demyelinating Lesions

Amit M. Saindane, Soonmee Cha, Meng Law, Xiaonan Xue,
Edmond A. Knopp, and David Zagzag

BACKGROUND AND PURPOSE: **Tumefactive demyelinating lesions (TDLs) can simulate intracranial neoplasms in clinical presentation and MR imaging appearance, and surgical biopsy is often performed in suspected tumors. Proton MR spectroscopy has been applied in assessing various intracranial diseases and is increasingly used in diagnosis and clinical management. Our purpose was to determine if multivoxel proton MR spectroscopy can be used to differentiate TDLs and high-grade gliomas.**

METHODS: **Conventional MR images, proton MR spectra, and medical records were retrospectively reviewed in six patients with TDLs diagnosed by means of biopsy or by documented clinical improvement, with or without supporting laboratory testing and follow-up imaging. Proton MR spectra of 10 high-grade gliomas with similar conventional MR imaging appearances were used for comparison. In contrast-enhancing, central, and perilesional areas of each lesion, peak heights of *N*-acetylaspartate (NAA), choline (Cho), and creatine (Cr) were measured and the lactate peak noted. Cho/Cr and NAA/Cr ratios of corresponding regions in TDLs and gliomas were compared.**

RESULTS: **No significant differences in mean Cho/Cr ratios were found in the corresponding contrast-enhancing, central, or perilesional areas of TDLs and gliomas. The mean central-region NAA/Cr ratio in gliomas was significantly lower than that of TDLs, but mean NAA/Cr ratios in other regions were not significantly different. A lactate peak was identified in four of six TDLs and three of 10 gliomas.**

CONCLUSION: **In the cases examined, the NAA/Cr ratio in the central region of TDLs and high-grade gliomas differed significantly. However, overall metabolite profiles of both lesions were similar; this finding emphasizes the need for the cautious interpretation of spectroscopic findings.**

Numerous reports in the literature describe large demyelinating lesions that masquerade as intracranial neoplasms. These so-called tumefactive demyelinating lesions (TDLs) can pose a considerable diagnostic challenge to both the clinician and the radiologist. Clinically, TDLs can cause symptoms suggestive of a mass lesion (1–6). On MR images, TDLs are often indistinguishable from high-grade glial neoplasms (2–8), demonstrating ill-defined borders, mass effect, perilesional edema, central necrosis, contrast enhancement, and variable involvement of gray matter structures. Even in the setting of established demyelinating disease such as multiple sclerosis (MS), the atypical appearance of a large lesion can suggest concurrent neoplasm (9–11).

The difficulty in diagnosing TDLs often leads to surgical biopsy, and the histopathologic findings can be misleading. The presence of hypercellularity, atypical reactive astrocytes, and mitotic figures can lead to a misdiagnosis of glial neoplasm, which can result in unnecessary and potentially harmful surgical resection or radiation therapy (2, 8). This diagnostic dilemma has prompted reports in the pathology literature that recommend the immunohistochemical evaluation for astrocyte and macrophage markers and the use of special stains for myelin and axons to correctly diagnose TDLs (2–4, 8).

Proton MR spectroscopy has been applied in the assessment of a variety of pathologic processes that affect the CNS, and it is increasingly being used to aid in diagnosis and clinical management. The metabolic alterations in primary CNS neoplasms (12–15) and in

Received October 8, 2001; accepted after revision April 12, 2002.

From the Department of Radiology (A.M.S., S.C., M.L., E.A.K.), Environmental Medicine (X.X.), Neurosurgery (E.A.K., D.Z.), Pathology (E.A.K., D.Z.), Division of Neuropathology, and the Kaplan Cancer Center (D.Z.), New York University Medical Center, 530 First Avenue, HCC-Basement, MRI Center, NY.

Address reprint requests to Soonmee Cha, MD, UCSF Medical Center, Department of Radiology, 505 Parnassus Ave., Box 0628, Rm L358, San Francisco, CA 94143.

demyelinating lesions of multiple sclerosis (MS) (16–20) have been studied extensively. Few studies, however, have been conducted to examine TDLs by using the technique (11, 21). Given their differences in pathophysiology, proton MR spectroscopy may be able to distinguish between TDLs and glial neoplasms, obviating surgical biopsy. Alternatively, proton MR spectroscopy may have problems similar to those of histopathologic analysis in differentiating these two lesions. The purpose of this retrospective study was to compare the proton MR spectroscopic findings of TDLs with those of histopathologically proven high-grade gliomas to noninvasively differentiate the two entities.

Methods

Patients

Approval for this study was obtained from the Institutional Board of Research Associates, and informed consent was obtained from all patients. In six patients with a single dominant intracranial mass lesion, TDLs were diagnosed either by biopsy or clinical follow-up, with or without supporting laboratory testing and follow-up imaging. Clinically, patients had an acute to subacute onset of signs or symptoms involving a focal neurologic deficit or increased intracranial pressure mimicking the findings of an intracranial neoplasm. Patients had no evidence of systemic illness, malignancy, or immunosuppression. The patients included two men and four women with an age range of 25–57 years and a mean age of 45.1 years.

For comparison, we selected 10 patients with high-grade intracranial gliomas that had similar conventional MR imaging features, that is, similar degrees of perilesional edema and mass effect, definite but varying degrees of contrast enhancement, and a predominant location in white matter. All gliomas were diagnosed by means of histopathologic examination after either stereotactic biopsy (in three patients) or surgical resection (in seven patients). The pathologic diagnoses were as follows: five anaplastic astrocytomas, one anaplastic oligodendroglioma, two anaplastic mixed gliomas, and two glioblastomas multiforme. These patients included nine men and one woman with an age range of 25–80 years with a mean age of 46.2 years.

MR Imaging

Imaging was performed on a 1.5-T clinical MR system (Siemens Medical Systems, Iselin, NJ). Localizing sagittal T1-weighted images were obtained, followed by axial T1-weighted (600/14/1 [TR/TE_{eff}/NEX]), T2-weighted (3400/119/1), and axial fluid-attenuated inversion recovery (9000/110/1/2200 [TR/TE_{eff}/NEX/TI]) images of the brain. Contrast-enhanced axial T1-weighted images were obtained after the administration of 0.1 mmol/kg gadopentetate dimeglumine. Conventional MR images were analyzed for lesion location, size, delineation, heterogeneity, mass effect, perilesional edema, necrosis or cyst formation, degree of contrast enhancement, and presence of additional lesions.

MR Spectroscopy

After the administration of gadopentetate dimeglumine for MR imaging, multivoxel 2D chemical-shift imaging (CSI) proton MR spectroscopy was performed. The volume of interest (VOI) was confirmed by obtaining half-Fourier–acquisition single-shot turbo spin-echo images (15/6/1/500 [TR/TE/NEX/TI]). In all patients, 10 axial, coronal, and sagittal images were obtained with 5-mm-thick sections and a 1 minute 15 second imaging time. A volume selective 2D CSI sequence with a TR/TE of 1500/144 was used for MR spectroscopy. The hybrid multivoxel CSI technique uses a point-resolved spectroscopy (PRESS) double spin-echo scheme for the preselection of a VOI that was usually defined to include the abnormality as well as normal brain tissue, when possible. To prevent the subcutaneous fat signals from providing a contribution to the spectra, the VOI was completely enclosed within the brain and positioned at the center of the phase-encoded field of view (FOV), which was large enough to prevent wraparound artifact. A typical VOI consisted of an 8×8-cm region placed within a 16×16-cm FOV on a 1.5–2-cm transverse section. A 16×16 phase-encoding matrix was used to obtain the 8×8 array of spectra in the VOI with an in-plane resolution of 1×1 cm and a voxel size of $1 \times 1 \times 1.5$ cm or $1 \times 1 \times 2$ cm, depending on the section thickness. The field homogeneity achieved in automated nonlocalized multiple angle projection shimming resulted in water peak line widths of typically less than 8 Hz in the VOI. The water signal intensity was suppressed with a 25.6-ms gaussian chemical shift selective excitation pulse followed by spoiler gradients. VOI selection and data collection were achieved with 5.12-ms sinc-hanning radio-frequency excitation and refocusing pulses. The second half of the second echo was collected by using 1024 data points and a spectral width of 1000 Hz. All multivoxel PRESS 2D CSI measurements included four preimages and one signal average acquisition, resulting in an acquisition time of 6 minutes 30 seconds. After the measurement and before data processing, the CSI grid was retrospectively adjusted to optimize voxel positioning over the lesion. The time domain data were multiplied with a gaussian filter function (center, 0 ms; half width, 256 ms), resulting in broadening of the spectral lines of less than 2 Hz.

All MR spectroscopy at our institution is performed after the administration of gadopentetate dimeglumine, primarily to examine areas of maximal enhancement and perienhancement T2 signal intensity. This practice is consistently applied; therefore, no interpatient or interstudy variation exists. Although the effect of gadopentetate dimeglumine on metabolite ratios is controversial, evidence suggests that, although the height of all peaks may be affected minimally, metabolite ratios are not substantially altered (22, 23).

The heights of selected metabolite peaks such as those of choline (Cho)-containing compounds, total creatine (Cr), *N*-acetylaspartate (NAA), and lactate (Lac) were measured. The metabolite peaks were assigned as follows: Cho, 3.21 ppm; Cr, 3.04 ppm; NAA, 2.02 ppm. Lac was identified at 1.33 ppm. Because a TE ranging from 135–144 optimizes the J coupling of Lac, inversion of the doublet at 1.33 ppm is sufficient to demonstrate Lac without having to demonstrate the doublet as an upright peak at a TE of 270 ms. Other metabolite peaks such as myo-inositol, lipids, and markers that peak at 2.1–2.6 ppm are visible by using a shorter TE, but they were not specifically examined because they are not as evident with the intermediate TE used. The peak height ratios for Cho/Cr and NAA/Cr were assigned in the area of maximum contrast enhancement, in the central region, in the perilesional nonenhancing T2 signal intensity abnormality, and in normal-appearing brain contralateral to the lesion. Additionally, the presence or absence of a Lac peak was confirmed in these four regions.

Statistical Analysis

Because of the small sample size, a normality assumption for Cho/Cr and NAA/Cr may not have been appropriate. Therefore, the data were summarized by using the median and range rather than mean and standard deviation. A nonparametric test for paired data, a Wilcoxon signed rank test was used to compare the Cho/Cr and NAA/Cr ratios in each region of the TDLs or gliomas with those of the contralateral normal-appearing brain. A Bonferroni correction was applied to account for multiple comparisons; therefore, a significance level of 5%/2, or 2 .5%, was used. A nonparametric test for independent samples, a Wilcoxon rank sum test, was used to compare

TABLE 1: MR imaging characteristics of tumefactive demyelinating lesions and glioma patients

Patient No.	Age (y)/Sex	Lesion	Lesion Size (cm)	Enhancement	Edema	Mass Effect	Necrosis/Cystic Degeneration	Lesion Delineation	Heterogeneity	Additional Lesions
1	50/F	TDL	2.9	50%	+++	+	Yes	Ill	Yes	No
2	46/F	TDL	1.7	30%	−	−	No	Well	No	Yes
3	25/M	TDL	1.8	10%	+	+	Yes	Ill	Yes	Yes
4	57/M	TDL	1.2	<5%	+	−	Yes	Ill	Yes	Yes
5	41/F	TDL	2.8	<5%	+	+	No	Ill	No	No
6	49/F	TDL	2.1	30%	+	+	Yes	Well	No	No
7	51/M	AA	2.7	50%	++	++	Yes	Intermediate	Yes	Yes
8	39/M	AA	1.4	90%	+	+	No	Ill	Yes	Yes
9	44/M	AO	4.3	50%	+++	+++	Yes	Ill	Yes	No
10	28/M	AA	1.9	90%	+	+	No	Ill	No	Yes
11	38/M	AMG	1.4	90%	++	+	No	Intermediate	No	No
12	38/M	AA	1.7	10%	+	+	Yes	Ill	Yes	Yes
13	80/M	AMG	3.5	80%	+	++	Yes	Well	Yes	No
14	25/F	AA	4.8	50%	++	++	Yes	Ill	Yes	No
15	60/M	GBM	2.3	80%	+	+	Yes	Ill	Yes	Yes
16	34/M	GBM	5.2	50%	+++	+++	Yes	Ill	Yes	Yes

Note.—TDL indicates tumefactive demyelinating lesion; AA, anaplastic astrocytoma; AO, anaplastic oligodendroglioma; AMG, anaplastic mixed glioma; GBM, glioblastoma multiforme.

Cho/Cr and NAA/Cr ratios between corresponding regions of TDLs and gliomas (eg, to compare the NAA/Cr ratio in the enhancing region of TDLs with the NAA/Cr ratio in the enhancing region of gliomas). A Bonferroni correction was applied to account for multiple comparisons; therefore, a significance level of 5%/4, 1 .25%, was used.

Results

Diagnosis of TDL

All patients in the TDL group received intravenous steroid therapy that resulted in a marked improvement in their symptoms. The diagnosis of TDL was made by means of stereotactic biopsy in one patient. Pathologically, extensive perivascular inflammatory infiltration was present, but no evidence of neovascularization was observed. Areas of hypercellularity were noted, as were atypical reactive astrocytes that could have been mistaken for a neoplastic process. Special stains for myelin and axons showed extreme myelin loss with relative preservation of the axonal architecture.

Five patients were treated conservatively and did not undergo biopsy because of a strong clinical suspicion and because of our previous experience with TDLs (24). In these patients, the diagnosis of TDL was made at clinical follow-up, with or without documented regression of the lesion on images. The time between initial MR imaging and final clinical follow-up ranged from 1.2 to 22.9 months, with a mean of 9.4 months. One patient developed positive somatosensory evoked potentials and had positive CSF test results for oligoclonal bands and myelin basic protein. The results of these tests were negative in the remaining four patients, but in these patients, the symptoms resolved or markedly improved. In one of these patients, follow-up images demonstrated complete resolution of the lesion, and in another, images obtained approximately 2 months after initial MR imaging demonstrated a considerable decrease in mass effect and contrast enhancement. None of the patients had a recurrence of symptoms or a worsening of imaging findings.

Conventional MR Imaging

MR imaging findings in TDLs and high-grade gliomas are summarized in Table 1. In the TDL group, four patients had lesions in the supratentorial white matter, whereas two patients had lesions in the brachium pontis. On T2-weighted images, the perilesional signal intensity abnormality was variable, but the images typically demonstrated mild to moderate edema and mass effect. TDLs demonstrated minimal to extensive contrast enhancement, and four had MR imaging findings consistent with necrosis or cyst formation or both. Three patients had evidence of additional smaller lesions. Representative MR images from a patient with biopsy-proved TDL are presented in Figure 1A and B.

In the high-grade glioma group, nine patients had lesions in the supratentorial white matter, whereas one patient had a lesion in the brain stem. All gliomas were contrast enhancing and demonstrated mild to marked perilesional edema and mass effect. Seven of the gliomas had MR imaging findings consistent with necrosis or cyst formation. Six patients had evidence of separate additional tumor foci. Representative MR images in a patient with a high-grade glioma are presented in Fig 2A and B.

MR Spectroscopy

Proton MR spectroscopic findings in TDLs and high-grade gliomas are summarized in Table 2. No significant differences in the mean Cho/Cr ratio were found between the corresponding enhancing, central, or perilesional regions of TDLs and gliomas. The mean NAA/Cr ratio in the central region of gliomas was significantly lower than that of the central region

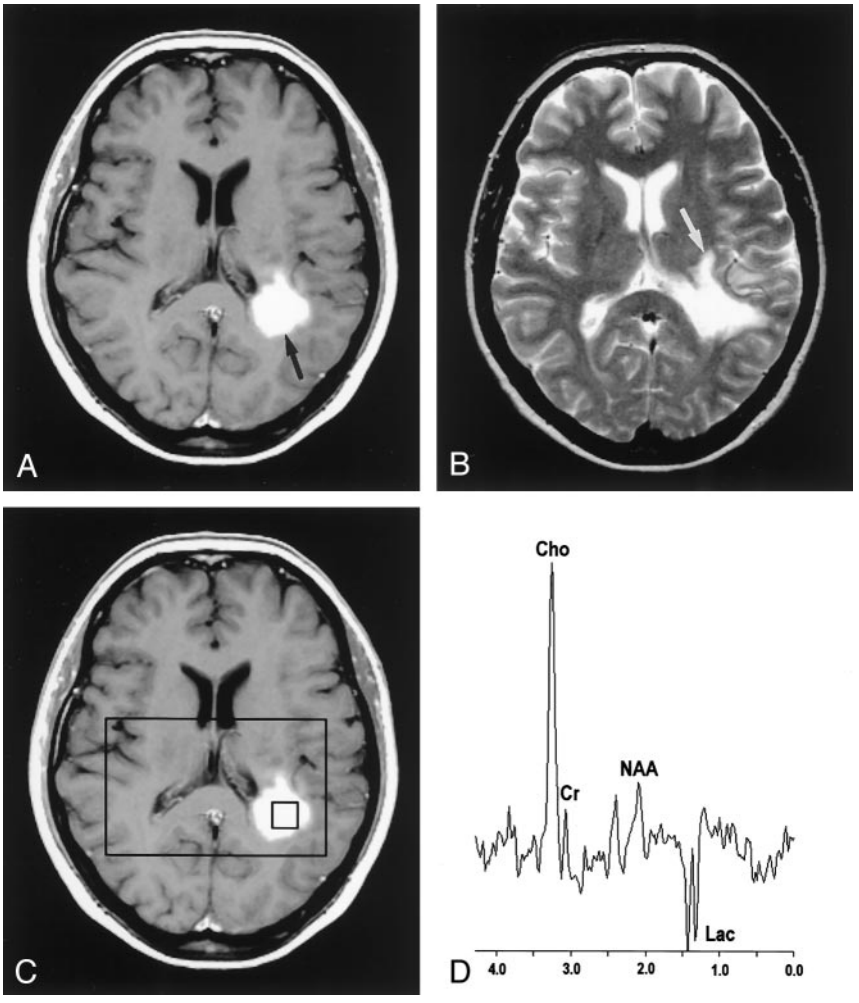

FIG 1. Images in a 50-year-old woman with biopsy-proven tumefactive demyelinating lesion.

A, Contrast-enhanced axial T1-weighted image (600/14/1) demonstrates an ill-defined enhancing mass (*arrow*) in the left frontoparietal periventricular white matter.

B, Axial T2-weighted image (3400/119/1) shows increased signal intensity (*arrow)* around the lesion.

C, Localizing image (600/14/1) for proton MR spectroscopy displays a voxel in the central portion of the lesion.

D, Proton MR spectrum obtained by using PRESS (1500/144) demonstrates an elevated Cho value, a decreased NAA value, and a Lac doublet.

of TDLs ($P = .008$). Although the difference in the mean NAA/Cr ratio approached significance, it was not significantly different in the corresponding enhancing regions of TDLs and gliomas ($P = .014$). No significant difference was found in the mean NAA/Cr ratio in the corresponding perilesional or normal regions of TDLs and gliomas. A Lac peak was identified in four of the six TDLs and in three of the 10 gliomas. Comparisons of mean Cho/Cr and NAA/Cr ratios between corresponding regions of TDLs and high-grade gliomas are summarized in Table 3.

Results of the comparison of the mean Cho/Cr and NAA/Cr ratios in TDLs and high-grade gliomas with those of contralateral normal-appearing brain are summarized in Table 4. In TDLs, although the mean Cho/Cr ratio approached the level of significance, it was not significantly different from that of contralateral normal-appearing brain in the enhancing ($P = .031$), central ($P = .031$), or perilesional ($P = .045$) regions. Likewise, the mean NAA/Cr ratio was not significantly different from that of the contralateral normal-appearing brain in the enhancing, central, or perilesional regions. A representative localizing image and an MR spectrum from a biopsy-proven TDL are presented in Figure 1C and D.

In high-grade gliomas, the mean Cho/Cr ratio was significantly elevated in all regions compared with contralateral normal-appearing brain. The NAA/Cr ratio was significantly decreased in the enhancing ($P = .006$) and central ($P = .007$) regions compared with contralateral normal-appearing brain. No significant difference in mean NAA/Cr ratio was found between the perilesional abnormality and contralateral normal-appearing brain ($P = .041$). A representative localizing image and an MR spectrum from a high-grade glioma are presented in Figure 2C and D.

Because of the extremely small number of TDLs examined, a formal statistical analysis to correlate the MR imaging features with the metabolite ratios from proton MR spectroscopy was considered inappropriate. In general, TDLs with more perilesional edema on T2-weighted images had lower NAA/Cr ratios than TDLs with less edema. A greater degree of enhancement on contrast-enhanced T1-weighted images was generally associated with a greater frequency of the Lac peak. TDLs with the MR imaging appearance of necrosis tended to have lower NAA/Cr ratios than TDLs without this appearance. No other noticeable relationships were present between conventional MR imaging features and metabolite ratios in TDLs. In the high-grade glioma group, no associations

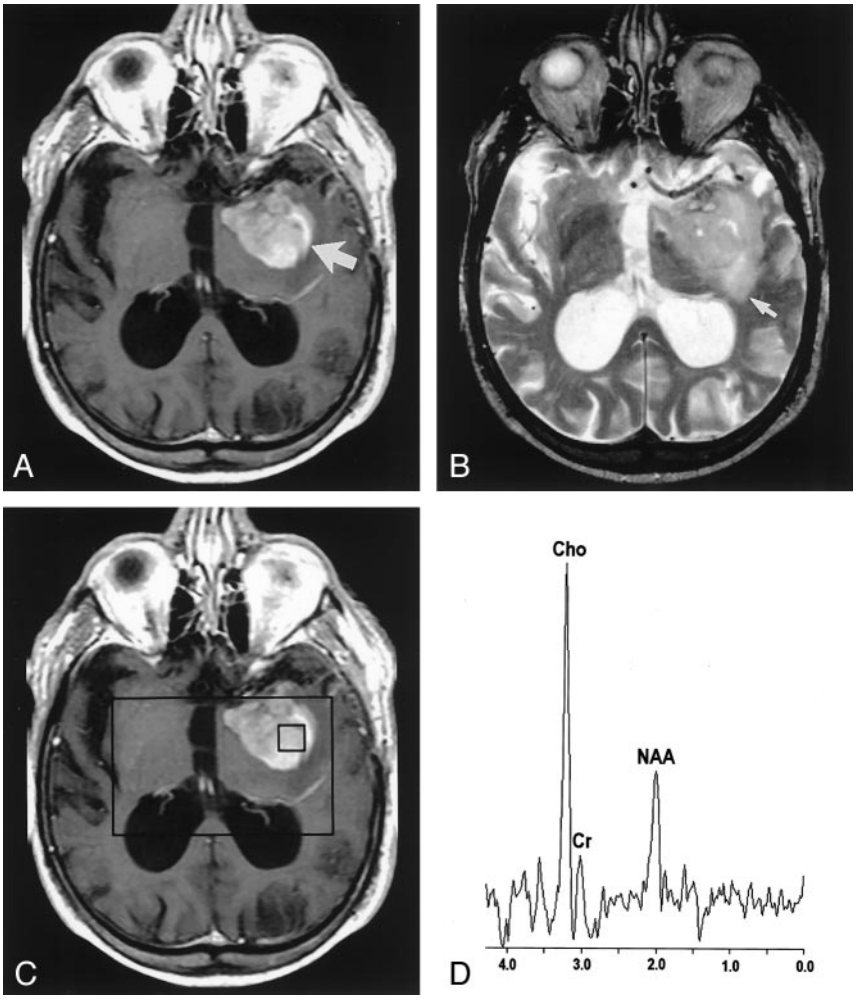

FIG 2. Images in an 81-year-old man with a high-grade mixed glioma.

A, Contrast-enhanced axial T1-weighted image (600/14/1) demonstrates an ill-defined enhancing mass (*arrow*) in the left temporal region.

B, Axial T2-weighted image (3400/119/1) shows increased signal intensity (*arrow*) around the lesion.

C, Localizing image (600/14/1) for proton MR spectroscopy displays a voxel in the central portion of the lesion.

D, Proton MR spectrum obtained by using PRESS (1500/144) demonstrates an elevated Cho value and a decreased NAA value.

between conventional MR imaging features and proton MR spectroscopy metabolites were obvious.

Discussion

The spectrum of primary demyelinating diseases of the CNS is composed of a variety of pathologic entities. MS, the most common form, is classically defined by a relapsing-remitting or progressive clinical course; the pathologic findings demonstrate multiple well-circumscribed lesions that lack mass effect or edema and that occur in characteristic locations such as the periventricular white matter (25). A subset of patients with demyelinating disease present with large solitary lesions with prominent edema and mass effect that produce clinical symptoms suggestive of a mass lesion (1–6). Most patients with these TDLs have single acute clinical attacks, and these generally do not progress to MS (26).

The MR imaging presentation of TDLs can mimic that of a high-grade glial neoplasm, resulting in a diagnostic dilemma (2–8). Both TDLs and high-grade gliomas can demonstrate ill-defined borders, extensive perilesional edema and mass effect, and the appearance of necrosis or cystic degeneration. Contrast enhancement on MR images is a nonspecific finding that reflects breakdown of the blood-brain barrier (BBB). This enhancement is commonly seen in TDLs because of inflammatory BBB breakdown and in high-grade gliomas because of an abnormal or absent BBB in newly formed capillaries.

Proton MR spectroscopy is a powerful technique that has been applied to the assessment of a variety of intracranial pathologic processes. In this study, we used proton MR spectroscopy to attempt to differentiate six TDLs from 10 high-grade gliomas that appeared similar on conventional MR images. We found that the only significant difference between TDLs and high-grade gliomas was the NAA/Cr ratio in the central region of the lesions. No other consistent differences in the metabolite profiles to discriminate the two types of lesions were present. An understanding of the pathologic basis for the metabolic alterations in demyelinating lesions and high-grade gliomas may, in part, explain our findings.

NAA is predominantly located in neurons (27) and is thus decreased in all neoplasms that cause the neurons to be displaced or replaced with malignant cells (12). Findings of numerous studies have demonstrated decreased NAA values in glial neoplasms (12–14). The Cho peak contains contributions from glycerophosphocholine, phosphocholine, and phos-

TABLE 2: MR spectroscopy characteristics of tumefactive demyelinating lesions and glioma patients

Patient No.	Lesion	Enhancing Region			Central Region			Perilesional T2 Region			Contralateral Normal Brain		
		Cho/Cr	NAA/Cr	Lac	Cho/Cr	NAA/Cr	Lac	Cho/Cr	NAA/Cr	Lac	Cho/Cr	NAA/Cr	Lac
1	TDL	4.6	1.0	++	3.5	1.0	++	1.7	1.2	+	0.5	1.6	−
2	TDL	1.8	1.9	+	3.0	3.2	++	1.6	2.9	+	0.9	1.6	−
3	TDL	1.7	0.7	−	4.9	2.3	+	1.9	1.2	−	0.7	1.6	−
4	TDL	2.4	1.3	−	3.3	2.7	−	1.5	0.3	−	0.8	2.0	−
5	TDL	2.8	1.9	−	1.6	2.5	−	1.4	2.6	−	1.4	3.0	−
6	TDL	1.7	1.7	+	2.3	1.4	−	1.1	1.7	−	0.9	1.9	−
7	AA	3.3	1.2	−	1.5	1.2	−	1.8	2.0	−	0.5	1.7	−
8	AA	3.3	0.7	−	9.0	1.1	−	1.0	0.9	−	0.7	1.2	−
9	AO	0.9	0.7	−	2.1	1.1	−	1.3	0.9	+	0.9	1.1	−
10	AA	4.3	0.9	−	3.8	0.8	−	2.0	1.4	−	0.7	1.7	−
11	AMG	2.5	0.6	−	2.5	0.6	−	2.0	1.3	−	1.6	3.6	−
12	AA	1.3	0.6	−	1.6	0.5	−	1.2	0.9	−	0.9	1.4	−
13	AMG	10.3	0.8	+	11.3	1.6	−	1.2	2.1	+	0.8	2.0	−
14	AA	12.7	0.6	−	4.7	0.8	+	1.5	1.3	−	1.1	1.5	−
15	GBM	1.8	0.7	−	2.2	0.9	−	1.5	1.2	−	1.0	1.5	−
16	GBM	10.0	1.0	−	4.4	0.8	−	2.3	1.0	−	1.2	2.1	−

Note.—TDL indicates tumefactive demyelinating lesion; AA, anaplastic astrocytoma; AO, anaplastic oligodendroglioma; AMG, anaplastic mixed glioma; GBM, glioblastoma multiforme.

TABLE 3: Comparison of spectroscopic characteristics of tumefactive demyelinating lesions and gliomas

Region		TDL (n = 6)		Glioma (n = 10)		*P* Value
		Median	Range	Median	Range	
Enhancing Region	Cho/Cr	2.1	1.7–4.6	3.3	0.9–12.7	.328
	NAA/Cr	1.5	0.7–1.9	0.7	0.6–1.2	.014
Central Region	Cho/Cr	3.2	1.6–4.9	3.2	1.5–11.3	.914
	NAA/Cr	2.4	1.0–3.2	0.9	0.5–1.6	.008
Perilesional T2 Region	Cho/Cr	1.6	1.1–1.9	1.5	1.0–2.3	.956
	NAA/Cr	1.5	0.3–2.9	1.3	0.9–2.1	.478
Contralateral Normal Brain	Cho/Cr	0.9	0.5–1.4	0.9	0.5–1.6	.621
	NAA/Cr	1.8	1.6–3.0	1.6	1.1–3.6	.383

Note.—Using the Wilcoxon rank-sum test and a Bonferroni correction for multiple comparisons, $P < .0125$ is considered statistically significant.

TABLE 4: Comparison of TDLs and gliomas with contralateral normal-appearing brain

	Region	Cho/Cr *P* Value	NAA/Cr *P* Value
TDL (n = 6)	Enhancing Region	.031	.094
	Central Region	.031	.400
	Perilesional T2 Region	.045	.293
Glioma (n = 10)	Enhancing Region	.007	.006
	Central Region	.006	.007
	Perilesional T2 Region	.006	.041

phatidylcholine, components that are thought to reflect cellular membrane density and turnover. As in any process that leads to hypercellularity and increased membrane proliferation, the Cho value is consistently elevated in gliomas (12–14). Some have even regarded the frequent coincidence of elevated Cho levels and decreased NAA levels in gliomas to be a tumor signature. The presence of Lac indicates that cellular respiration has shifted from the oxidative metabolism of carbohydrates to nonoxidative metabolism. Increased reliance on anaerobic glycolysis is found in highly malignant tumors (15), and is thought to result from hypercellular and hypermetabolic lesions that outgrow their blood supply.

Although TDLs may represent a clinical entity separate from MS (26), analogies may reasonably be drawn from their similar pathologic features. The acute lesion of MS is associated with the breakdown of the BBB and is pathologically characterized by a dense perivascular inflammatory infiltrate that contributes to demyelination and axonal damage (28). TDLs also demonstrate a perivascular infiltration of inflammatory cells and demyelination with relative sparing of axonal processes (6, 8, 26). Few prior studies have specifically addressed the proton MR spectroscopic features of TDLs; however, numerous studies have been conducted to examine the spectroscopic findings in the demyelinating lesions of MS (16–20).

Elevation of the Cho level is consistently found in acute MS lesions (17–20). Explanations for this finding have included reactive astrogliosis, demyelination, and inflammation. Intense reactive astrogliosis has long been recognized in acute MS lesions, and because Cho-containing compounds are predominantly located in glial cells (27), membrane turnover in pro-

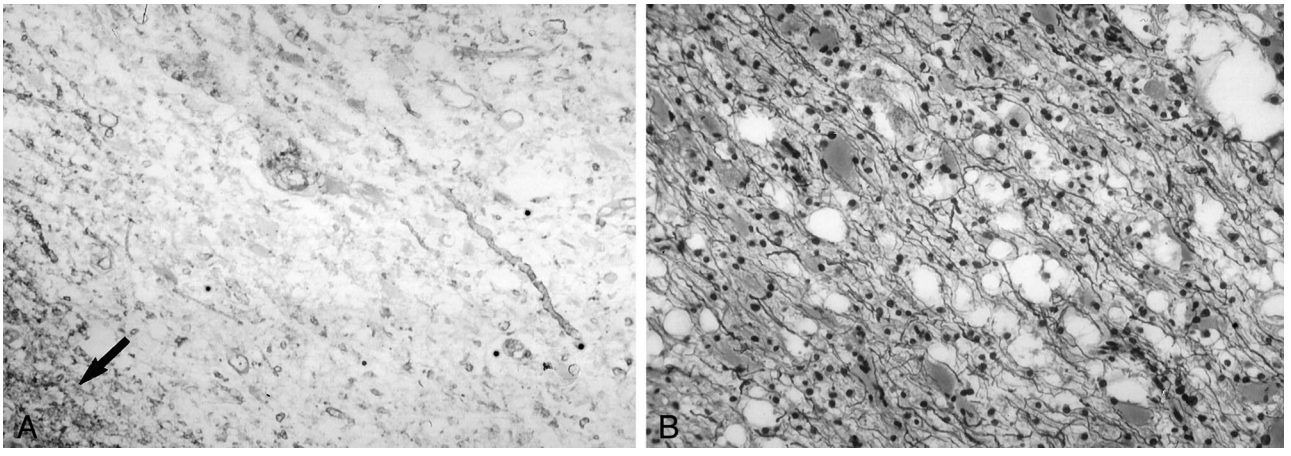

FIG 3. Photomicrographs of a biopsy specimen from a tumefactive demyelinating lesion in a 50-year-old woman. *Left*, A Luxol fast blue stain demonstrates extensive myelin loss. The lower left corner (*arrow*) shows a relatively normal pattern of myelination. *Right*, Silver stain demonstrates relative preservation of axis cylinders.

liferating astrocytes could possibly lead to increased Cho levels. Support for this hypothesis comes from the study by Bitsch et al (20), who at neuropathologic correlation found that an elevation of the Cho value corresponded with glial proliferation. Evidence against demyelination as a cause for Cho elevation comes from the study by Brenner et al (29), who found elevated Cho levels in the acute plaques of experimental allergic encephalitis (EAE), in which intense inflammation but no demyelination occurs. The findings of this study suggest that inflammation alone could lead to elevated Cho levels in EAE, possibly secondary to the import of the enzyme choline oxidase in infiltrating macrophages and lymphocytes.

Another common finding in the acute MS lesion is reduced NAA levels (17–20, 30). Axonal damage and neuronal mitochondrial dysfunction have both been implicated. In pathologically confirmed acute MS lesions, evidence shows early axonal degeneration (19) and decreased axonal density (20) that is associated with decreased NAA values. The reduction in NAA has been found to be reversible over time in some lesions (18); this finding suggests that decreased mitochondrial NAA synthesis from transient neuronal dysfunction (29) may be at least partly responsible.

A more variable finding in the acute lesion of MS is the presence of Lac (17–20, 31). Local ischemia, neuronal mitochondrial dysfunction, and inflammation have all been proposed as possible mechanisms. Ischemia from elevated intralesional pressure could explain the increase in Lac; however, no pathologic evidence of ischemia exists (19). Alternatively, neuronal mitochondrial dysfunction could lead to increased Lac production due to neuronal glycolysis (29). Enhancing lesions have demonstrated substantially greater Lac signal frequency than nonenhancing lesions (31), and pathologically, the highest Lac is found in plaques with high inflammatory activity (20); this finding suggests that elevated Lac values may be related to inflammation. Further support for this hypothesis comes from in vitro studies that demonstrate increased glucose utilization and Lac production in activated macrophages (32).

In this study, no significant difference in mean Cho/Cr ratio was found between corresponding regions of TDLs and high-grade gliomas. Because Cho is a marker for cellular membrane turnover that is not specific to neoplastic processes, similar elevations in the metabolite could possibly result from astroglial proliferation in TDLs and neoplastic growth in high-grade gliomas. This intense astrogliosis, along with hypercellularity, nuclear pleomorphism, and mitotic activity has, in some cases, led to the histopathologic misdiagnosis of TDLs as gliomas (8). Our patient with a biopsy-proven TDL had atypical reactive astrocytes that could have easily been mistaken for a neoplastic process. As demonstrated in Figure 3, the presence of demyelination with relative axonal sparing on special stains for myelin and axons allowed for a definitive diagnosis of TDL.

Comparison of the NAA/Cr ratio between TDLs and high-grade gliomas demonstrated a significant difference only in the corresponding central portions of the lesions. In most high-grade gliomas in this study, MR images showed central necrosis. This appearance is histopathologically correlated with necrosis of the brain parenchyma, including the neuronal elements (33, 34); this observation explains the marked decrease in NAA levels in the central portion of gliomas. Four TDLs in this study demonstrated the appearance of necrosis or cystic degeneration on MR images; these lesions generally had NAA/Cr ratios that were lower than the ratios in those without necrosis. At histopathologic analysis, cystic degeneration and areas of micronecrosis may be seen in TDLs, but extensive coagulative necrosis is rarely observed (8). NAA/Cr ratios are acutely decreased in TDLs, indicating that some degree of axonal damage or dysfunction is occurring. However, because some TDLs demonstrate complete resolution on follow-up images, the extent of neuronal damage or death in the center of TDLs is unlikely to match that found in the center of high-grade gliomas; this concept may possibly explain the difference in their NAA/Cr ratios.

The mean Cho/Cr ratio in all regions of TDLs was not significantly different from that of normal-ap-

pearing contralateral brain. In some patients, however, the Cho/Cr ratio demonstrated a prominent elevation, which suggested that different degrees of inflammation or membrane proliferation in reactive astrocytes may be occurring in different lesions. The mean NAA/Cr ratio in all regions of TDLs was not significantly different from that of normal-appearing contralateral parts of the brain. A prominent decrease in NAA values was observed in some patients, suggesting that, across all TDLs, different degrees of axonal damage or dysfunction may be occurring or that the lesions were at different stages in their evolution. As has been found in some MS lesions, an initial transient decrease in NAA may occur with subsequent normalization (18). The wide variations in peak heights in different TDLs and the small number of cases examined could explain the lack of significant differences in mean peak ratios between regions in TDLs and those in contralateral areas of normal-appearing brain. This high degree of variability in metabolite ratios in TDLs underscores the problems in the use of proton MR spectroscopy for discriminating between TDLs and gliomas.

A Lac peak was present in four of six TDLs. Interestingly, the two TDLs without a Lac peak had only minimal contrast enhancement on MR images. Nesbit et al (25) found that contrast enhancement in MS lesions reflects the degree of macrophage infiltration. In of our four TDLs with Lac peaks, the relative peak height of the Lac doublet appeared to depend on the degree of contrast enhancement; this finding suggested that BBB breakdown and inflammation may be related to the elevation of Lac levels in TDLs.

We must stress that the diagnosis of demyelinating disease was based on clinical but not necessarily imaging-documented follow-up. Although we cannot be absolutely certain that patients who did not undergo biopsy had TDLs, the clinical behavior of the lesions and, in some cases, the laboratory and radiologic follow-up findings were highly atypical for high-grade gliomas. The presence of other episodes of neurologic dysfunction would have made the diagnosis of demyelinating disease more certain; however, patients presenting with TDLs typically have only single clinical attacks. A longer period of clinical and radiologic follow-up would be helpful in confirming the diagnosis of TDL in patients without a histopathologic diagnosis. Although other demyelinating diseases such as progressive multifocal leukoencephalopathy (26, 35) and acute disseminated encephalomyelitis (26) can also sometimes appear as large solitary mass lesions, clinical and imaging features of these processes are usually present to allow for their discrimination.

Two previous groups have described the proton MR spectroscopic features of TDLs. One found that a tumefactive MS lesion demonstrated slightly elevated Cho levels, decreased NAA levels, and an excess of Lac and lipids (11). Another used linear discriminant analysis and pattern recognition to distinguish five TDLs from 66 gliomas (21). With the exception of the NAA/Cr ratio in the central portions of the lesions, the results of our study showed that the metabolite profiles of TDLs and high-grade gliomas had no appreciable differences. Some studies have revealed that the MR spectra in perilesional areas of noninfiltrating processes such as metastases and abscesses are relatively normal, whereas those in the perilesional areas of infiltrating gliomas are abnormal (36, 37). Although this finding could be extrapolated to include TDLs, in the heterogeneous and limited number of cases examined in this study, we did not find any significant differences between the metabolite ratios of perilesional areas in TDLs and high-grade gliomas.

Although the pathogenesis of acute demyelinating lesions and that of high-grade glial neoplasms are vastly different, both result in some degree of rapid cellular proliferation, increased metabolism, and disruption of the native neuronal tissue. These similar metabolic features, combined with the heterogeneous and evolving nature of the lesions, could result in substantial overlap in the spectroscopic findings. In fact, one of the patients in this study had undergone biopsy for definitive diagnosis because of a proton MR spectroscopic profile that was highly suggestive of a tumor (as shown in Figure 1D).

A potential criticism of this study is the use of semiquantitative peak heights instead of peak areas. Although a quantitation of the peak areas would have yielded more precise values, the overall conclusions of the study are unlikely to have been affected. One major limitation of this study is the small number of TDLs examined and therefore its limited statistical power. Although a larger number of cases could potentially lead to other significant differences in metabolite ratios between TDLs and gliomas, the findings of this study show that the distinction between the spectroscopic tumor signature and the spectrum found in TDLs may not always be clear. Given the results of this study, we believe that the MR spectra in suspected tumors should be interpreted with caution. This study also underscores the need to include demyelinating lesions in the differential diagnosis of neoplasms of the brain.

Conclusion

Proton MR spectroscopy is a powerful noninvasive tool for understanding the biochemical alterations in various intracranial disease processes. In this study, we found that high-grade gliomas and TDLs share many similar features at both conventional MR imaging and proton MR spectroscopy. Except for significant differences in the NAA/Cr ratio in their central regions, no other metabolite ratios could be used to distinguish high-grade gliomas and TDLs with confidence; this finding emphasizes the need for the cautious interpretation of spectroscopic findings.

Acknowledgments

We acknowledge the assistance of Nouha Salibi from Siemens Medical Systems for technical support.

References

1. Mastrostefano R, Occhipinti E, Bigotti G, et al. **Multiple sclerosis plaque simulating cerebral tumor: case report and review of the literature.** *Neurosurgery* 1987;21:244–246
2. Hunter SB, Ballinger WE Jr, Rubin JJ. **Multiple sclerosis mimicking primary brain tumor.** *Arch Pathol Lab Med* 1987;111:464–468
3. Giang DW, Poduri KR, Eskin TA, et al. **Multiple sclerosis masquerading as a mass lesion.** *Neuroradiology* 1992;34:150–154
4. Silva HC, Callegaro D, Marchiori PE, et al. **Magnetic resonance imaging in five patients with a tumefactive demyelinating lesion in the central nervous system.** *Arq Neuropsiquiatr* 1999;57:921–926
5. Kalyan-Raman UP, Garwacki DJ, Elwood PW. **Demyelinating disease of corpus callosum presenting as glioma on magnetic resonance scan: a case documented with pathological findings.** *Neurosurgery* 1987;21:247–250
6. Dagher AP, Smirniotopoulos J. **Tumefactive demyelinating lesions.** *Neuroradiology* 1996;38:560–565
7. Kurihara N, Takahashi S, Furuta A, et al. **MR imaging of multiple sclerosis simulating brain tumor.** *Clin Imaging* 1996;20:171–177
8. Zagzag D, Miller DC, Kleinman GM, et al. **Demyelinating disease versus tumor in surgical neuropathology: Clues to a correct pathological diagnosis.** *Am J Surg Pathol* 1993;17:537–545
9. Nahser HC, Vieregge P, Nau HE, et al. **Coincidence of multiple sclerosis and glioma: clinical and radiological remarks on two cases.** *Surg Neurol* 1986;26:45–51
10. Khan OA, Bauserman SC, Rothman MI, et al. **Concurrence of multiple sclerosis and brain tumor: clinical considerations.** *Neurology* 1997;48:1330–1333
11. Ernst T, Chang L, Walot I, et al. **Physiologic MRI of a tumefactive multiple sclerosis lesion.** *Neurology* 1998;51:1486–1488
12. Usenius JP, Kauppinen RA, Vainio PA, et al. **Quantitative metabolite patterns of human brain tumors: detection by 1H NMR spectroscopy in vivo and in vitro.** *J Comput Assist Tomogr* 1994;18:705–713
13. Poptani H, Gupta RK, Roy R, et al. **Characterization of intracranial mass lesions with in vivo proton MR spectroscopy.** *AJNR Am J Neuroradiol* 1995;16:1593–1603
14. Shimizu H, Kumabe T, Tominaga T, et al. **Noninvasive evaluation of malignancy of brain tumors with proton MR spectroscopy.** *AJNR Am J Neuroradiol* 1996;17:737–747
15. Barker PB, Glickson JD, Bryan RN. **In vivo magnetic resonance spectroscopy of human brain tumors.** *Top Magn Reson Imaging* 1993;5:32–45
16. Grossman RI, Lenkinski RE, Ramer KN, et al. **MR proton spectroscopy in multiple sclerosis.** *AJNR Am J Neuroradiol* 1992;13:1535–1543
17. Arnold DL, Matthews PM, Francis GS, et al. **Proton magnetic resonance spectroscopic imaging for metabolic characterization of demyelinating plaques.** *Ann Neurol* 1992;31:235–441
18. Davie CA, Hawkins CP, Barker GJ, et al. **Serial proton magnetic resonance spectroscopy in acute multiple sclerosis lesions.** *Brain* 1994;117:49–58
19. Silver NC, Barker RA, MacManus DG, et al. **Proton magnetic resonance spectroscopy in a pathologically confirmed acute demyelinating lesion.** *J Neurol* 1997;244:204–207
20. Bitsch A, Bruhn H, Vougioukas V, et al. **Inflammatory CNS demyelination: histopathologic correlation with in vivo quantitative proton MR spectroscopy.** *AJNR Am J Neuroradiol* 1999;20:1619–1627
21. De Stefano N, Caramanos Z, Preul MC, et al. **In vivo differentiation of astrocytic brain tumors and isolated demyelinating lesions of the type seen in multiple sclerosis using 1H magnetic resonance spectroscopic imaging.** *Ann Neurol* 1998;44:273–278
22. Lin AP, Ross BD. **Short-echo time proton MR spectroscopy in the presence of gadolinium.** *J Comput Assist Tomogr* 2001;25:705–712
23. Smith JK, Kwock L, Castillo M. **Effects of contrast material on single-volume proton MR spectroscopy.** *AJNR Am J Neuroradiol* 2000;21:1084–1089
24. Cha S, Pierce S, Knopp EA, et al. **Dynamic contrast-enhanced T2*-weighted MR imaging of tumefactive demyelinating lesions.** *AJNR Am J Neuroradiol* 2001;22:1109–1116
25. Nesbit GM, Forbes GS, Scheithauer BW, et al. **Multiple sclerosis: histopathologic and MR and/or CT correlation in 37 cases at biopsy and three cases at autopsy.** *Radiology* 1991;180:467–474
26. Kepes JJ. **Large focal tumor-like demyelinating lesions of the brain: intermediate entity between multiple sclerosis and acute disseminated encephalomyelitis? A study of 31 patients.** *Ann Neurol* 1993;33:18–27
27. Urenjak J, Williams SR, Gadian DG, et al. **Proton nuclear magnetic resonance spectroscopy unambiguously identifies different neural cell types.** *J Neurosci* 1993;13:981–989
28. Trapp BD, Peterson J, Ransohoff RM, et al. **Axonal transection in the lesions of multiple sclerosis.** *N Engl J Med* 1998;338:278–285
29. Brenner RE, Munro PM, Williams SC, et al. **The proton NMR spectrum in acute EAE: the significance of the change in the Cho:Cr ratio.** *Magn Reson Med* 1993;29:737–745
30. Bruhn H, Frahm J, Merboldt KD, et al. **Multiple sclerosis in children: cerebral metabolic alterations monitored by localized proton magnetic resonance spectroscopy in vivo.** *Ann Neurol* 1992;32:140–150
31. Simone IL, Tortorella C, Federico F, et al. **Axonal damage in multiple sclerosis plaques: a combined magnetic resonance imaging and 1H-magnetic resonance spectroscopy study.** *J Neurol Sci* 2001;182:143–150
32. Lopez-Villegas D, Lenkinski RE, Wehrli SL, et al. **Lactate production by human monocytes/macrophages determined by proton MR spectroscopy.** *Magn Reson Med* 1995;34:32–38
33. Tovi M, Hartman M, Lilja A, et al. **MR imaging in cerebral gliomas.** Tissue component analysis in correlation with histopathology of whole-brain specimens. *Acta Radiol* 1994;35:495–505
34. Dean BL, Drayer BP, Bird CR, et al. **Gliomas: classification with MR imaging.** *Radiology* 1990;174:411–415
35. Vanneste JA, Bellot SM, Stam FC. **Progressive multifocal leukoencephalopathy presenting as a single mass lesion.** *Eur Neurol* 1984;23:113–118
36. Burtscher IM, Skagerberg G, Geijer B, et al. **Proton MR spectroscopy and preoperative diagnostic accuracy: an evaluation of intracranial mass lesions characterized by stereotactic biopsy findings.** *AJNR Am J Neuroradiol* 2000;21:84–93
37. Law M, Cha S, Knopp EA, et al. **High-grade gliomas and solitary metastases: differentiation by using perfusion and proton spectroscopic MR imaging.** *Radiology* 2002;222:715–721